arXiv:1607.02375v1 [physics.atm-clus] 8 Jul 2016

Sub-picosecond energy transfer from a highly intense THz pulse to water: a computational study based on the TIP4P/2005 model.

Pankaj Kr. Mishra,[1, 2, 3, a)] Oriol Vendrell,[1, 2, b)] and Robin Santra[1, 2, 3]

[1)] *Center for Free-Electron Laser Science, DESY, Notkestraße 85, D-22607 Hamburg, Germany*

[2)] *The Hamburg Centre for Ultrafast Imaging, Luruper Chaussee 149, D-22761 Hamburg, Germany*

[3)] *Department of Physics, University of Hamburg, Jungiusstraße 9, D-20355 Hamburg, Germany*

The dynamics of ultrafast energy transfer to water clusters and to bulk water by a highly intense, sub-cycle THz pulse of duration $\approx$ 150 fs is investigated in the context of force-field molecular dynamics simulations. We focus our attention on the mechanisms by which rotational and translational degrees of freedom of the water monomers gain energy from these sub-cycle pulses with an electric field amplitude of up to about 0.6 V/Å. It has been recently shown that pulses with these characteristics can be generated in the laboratory [PRL 112, 213901 (2014)]. Through their permanent dipole moment, water molecules are acted upon by the electric field and forced off their preferred hydrogen-bond network conformation. This immediately sets them in motion with respect to one another as energy quickly transfers to their relative center of mass displacements. We find that, in the bulk, the operation of these mechanisms is strongly dependent on the initial temperature and density of the system. In low density systems, the equilibration between rotational and translational modes is slow due to the lack of collisions between monomers. As the initial density of the system approaches 1 g/cm^3, equilibration between rotational and translational modes after the pulse becomes more efficient. In turn, low temperatures hinder the direct energy transfer from the pulse to rotational motion owing to the resulting stiffness of the hydrogen bond network. For small clusters of just a few water molecules we find that fragmentation due to the interaction with the pulse is faster than equilibration between rotations and translations, meaning that the latter remain colder than the former after the pulse. In contrast, clusters with more than a few tens of water molecules already display energy gain dynamics similar to water in condensed phases owing to inertial confinement of the internal water molecules by the outer shells. In these cases, a complete equilibration becomes possible.

[a)] pankaj.kumar.mishra@desy.de

[b)] oriol.vendrell@cfel.de

I. INTRODUCTION

Water in its liquid form is the universal solvent in which most chemical processes in a biological environment take place. For this reason, its properties under variations of thermodynamic parameters such as temperature[1] and pressure[2], under external perturbations such as electric fields[3,4] and ultrasound waves[5], or under confinement[6–11] have been the subject of much attention. Isolated water molecules have a permanent dipole moment of 1.85 D[12], which varies with cluster size and converges to 2.85 D for liquid water[13]. In the presence of an electric field, the permanent dipole of the water monomers experience a torque, which tries to orient the water dipole along the polarization direction of the field and perturbs the equilibrium arrangement formed by the hydrogen bond (H-bond) network[14]. For example, a DC or slowly varying electric field with an amplitude in the range of 0.5×10^7-10×10^7 V/cm can induce structural transformations in water clusters and modify their equilibrium geometry from ring-like to chain-like structures [15–19]. These changes are linked to a reduction of the average number of H-bonds in the system. Strong electric fields polarize the electronic cloud and lead to modifications of the dipole moment of the water monomers. These changes are dependent on cluster size and field strength[20]. Other static properties of bulk water like its diffusion constant[14,16] or its intramolecular vibrational frequencies[17] can also be altered by the structural modifications caused by the presence of electric fields. Electric fields can also have an effect on the mechanism of biological processes occurring in liquid water. Examples include the modification of rate constant of folding and unfolding processes of proteins and peptides[21–23] and of other types of chemical reactions[24,25].

Laser sources have also been applied to induce structural[26,27] and dynamical[28,29] modifications in liquid water. Femtosecond laser pulses can be tuned to the excitation of internal degrees of freedom of the water monomers, e.g. vibrational modes[30,31]. Specifically, infrared (IR) lasers can directly excite the intramolecular O-H stretching modes, which strongly absorb at wavenumbers $1/\lambda \approx 3500$ cm^{-1}. After the pulse, the energy deposited by the laser pulse relaxes via vibrational energy redistribution to other intramolecular and intermolecular vibrational modes[32–35]. Alternatively, sub-cycle and highly intense THz pulses can also transfer a large amount of energy to liquid water, which can be the equivalent of several hundreds of degrees Kelvin[36,37]. The mechanism by which the sub-cycle THz pulse interacts with the medium is off resonance with intramolecular degrees of freedom and with libra-

tional modes of bulk water[37] and more closely related to the interaction mechanism of water molecules with DC fields.

In this work, we investigate the interaction of intense, sub-cycle THz pulses with water clusters of various sizes and with bulk water at a range of initial temperatures and densities. The pulses considered are characterized by peak electric field amplitudes of up to 0.6 V/Å. Pulses of similar peak field amplitude in the frequency range of 1-10 THz have recently been demonstrated using non-linear organic crystals[38]. Our simulations are based on the TIP4P/2005 rigid water model[39]. Compared to preceding studies of THz-pumped liquid water based on *ab initio* molecular dynamics (AIMD) simulations[36,37], which were performed on much smaller simulation boxes and for very specific initial conditions, the use of a parametrized force field allows for a systematic investigation of the transition from cluster to bulk behavior and of a wide range of initial temperatures and densities. We first concentrate on the interaction of the THz pulse with one isolated water molecule and with clusters of a few water molecules. Based on these simulations we discuss the basic mechanism by which the THz pulse initially transfers energy to the system and how this energy is transferred among the hindered rotational and translational modes of nearby interacting water molecules. Subsequently, we discuss the interaction of bulk water at various initial temperatures and densities under periodic boundary conditions at constant volume and particle number. This means, essentially, that some form of external confinement of the water molecules in the interaction volume with the THz pulse is being assumed. This can correspond to a macroscopic confinement of the whole interaction region by hard walls that keep the system from expanding as it heats up, or it can correspond to inertial confinement of the region of a bulk system crossed by the pump pulse. By simulating clusters with up to several thousands of water molecules, we establish that indeed the system is inertially confined as it heats up. Since the energy intake proceeds on a sub-picosecond time scale, the inner regions of the cluster remain essentially at their initial density throughout the confinement exerted by the outer shells, which need a longer time to start moving away from the cluster. For periodic systems at low density and high temperature, the behavior of isolated water molecules is recovered, whereas at a density of 1 g/cm^3 the amount of energy gained by the system is found to be strongly dependent on the initial temperature, which determines the average strength of the hydrogen bonds.

The structure of the paper is as follows. Section II describes the computational methods.

Section III A discusses the interaction of the THz pulse with water clusters and the transition to bulk behavior. Section III B describes the response of bulk water at different initial temperatures and densities to the THz pulse, and Section IV concludes and provides some outlook.

II. COMPUTATIONAL DETAILS

Simulations of the water clusters and of bulk water under periodic boundary conditions were performed with the Large-scale Atomic/Molecular Massively Parallel Simulator (LAMMPS)[40] using the rigid TIP4P/2005 water force field model[39]. For the water cluster simulations, 1000 initial atomic configurations and velocities were generated from a long molecular dynamics (MD) trajectory performed under canonical (NVT) conditions and equilibrated at 200 K. Different sets of initial conditions were sampled with a 10 ps time interval to avoid artificial correlations between each sampled phase space point. The Nose-Hoover thermostat[41,42] was used to maintain the temperature for the phase space sampling NVT trajectory. Each set of 1000 initial conditions was then propagated microcanonically for 1.5 ps in the presence of the THz pulse. For all trajectory propagations the velocity-Verlet algorithm was used with a time step of 1 fs. A cut-off radius of 15 Å was used for the calculation of the short-range Lennard-Jones interactions. Water clusters of sizes 1, 2, 4, 8, 32 and 64 monomers were initially considered. In order to study the effect of inertial confinement, a bigger spherical cluster with 8843 water molecules and radius $\approx$ 50 Å was equilibrated at 300 K and subsequently exposed to the THz pulse. All water cluster simulations were performed with non-periodic boundaries in all directions.

Bulk water simulations at different initial temperatures and densities were based on thermally equilibrated cubic boxes containing 2048 water molecules. By selecting the box size, a range of initial densities of 1.0 g/cm^3, 0.296 g/cm^3, 0.064 g/cm^3 and 0.019 g/cm^3 were considered. Each box was then equilibrated at different temperatures of 200 K, 300 K, 400 K, 500 K and 600 K. Each set of initial density and temperature conditions was subsequently propagated microcanonically for 1.5 ps in the presence of the THz pulse.

The same half cycle THz pulse profile as in previous investigations was considered here[36,37]. The THz pump pulse is given by

$$\mathbf{E}(t) = \epsilon(t)\mathbf{u}_z \cos(\omega_c t + \phi), \tag{1}$$

where $\epsilon(t) = A\exp\{-(t-t_0)^2/2\sigma^2\}$ is a Gaussian envelope with $\sigma = 84.93$ fs. This corresponds to a full width at half maximum (fwhm) of $\epsilon^2(t)$ of 141 fs. The maximum electric field amplitude $A = 0.61$ V/Å corresponds to a power per unit area of 5×10^{12} W/cm^2. The mean photon frequency considered is $\omega_c = 2\pi \times 3$ THz (100 cm^{-1}) which results in a pulse between a half and a full cycle long. $\mathbf{u}_z$ is the polarization direction of the electric field and ϕ is the carrier to envelope phase which is set to $\pi/2$. By convention, the THz pulse envelope is centered at $t_0 = 0$ in all simulations and microcanonical trajectories start at $t = -250$ fs.

The analysis of the energy gain by water clusters and bulk water is performed on the basis of decomposing the total kinetic energy ($E_K^{(m)}$) of each rigid water monomer m in terms of its rotational energy ($E_R^{(m)}$) and translational energy ($E_T^{(m)}$) components. This is simply achieved in Cartesian coordinates by,

$$E_T^{(m)} = \frac{|\sum_{a_m} M_{a_m}\mathbf{V}_{a_m}|^2}{2\sum_{a_m} M_{a_m}} \tag{2}$$

and

$$\begin{aligned} E_R^{(m)} &= \sum_{a_m} \frac{\mathbf{j}_{a_m}^2}{2M_{a_m}|\mathbf{x}_{a_m}|^2} \\ \mathbf{j}_{a_m} &= M_{a_m}(\mathbf{x}_{a_m} \times \mathbf{v}_{a_m}), \end{aligned} \tag{3}$$

where $\mathbf{x}_{a_m} \equiv \mathbf{X}_{a_m} - \mathbf{X}_m$ and $\mathbf{v}_{a_m} \equiv \mathbf{V}_{a_m} - \mathbf{V}_m$ define the position and velocity of atom a in monomer m relative to the center of mass position $\mathbf{X}_m$ and velocity $\mathbf{V}_m$ of the monomer, respectively. In general, at this point the kinetic energy per monomer related to vibrational motion of the remaining $3N-6$ intramolecular coordinates $E_V^{(m)} = E_K^{(m)} - E_T^{(m)} - E_R^{(m)}$ can be obtained. In the present case, owing to the rigid nature of the water model used, $E_V^{(m)} = 0$. In particular, the intramolecular degrees of freedom were kept fixed in LAMMPS by the SHAKE algorithm[43].

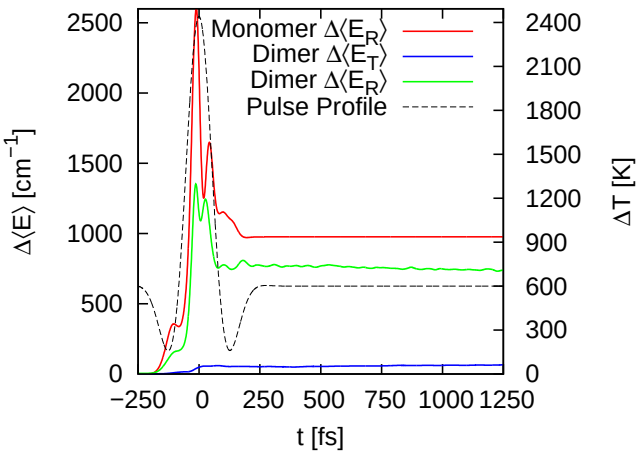

FIG. 1. Translational ($\Delta\langle E_T\rangle$) and rotational ($\Delta\langle E_R\rangle$) energy increase per water monomer for the monomer and dimer cases. On the right axis the kinetic temperature $T = \frac{2E}{3k}$ with k the Boltzmann factor is shown. The THz pulse profile appears as a dotted line.

III. RESULTS AND DISCUSSION

A. Interaction of the THz pulse with water clusters

1. Water monomer and dimer

The effect of the THz pulse on a single water monomer and on the water dimer is analyzed first. The ensemble averaged translational $\langle E_T\rangle$ and rotational $\langle E_R\rangle$ energies per monomer were obtained by averaging over 1000 initial configurations and velocities. In the case of the monomer and due to the intramolecular constraints, the sampling of initial conditions generates only random orientations and angular velocities of the water molecule, the latter being compatible with a target temperature of 200 K. In the dimer case, overall rotations of the system as well as intermolecular coordinates are sampled according to the target temperature of 200 K. The electric field is polarized along the z-axis in all simulations. Due to the electroneutrality of the isolated water monomer, only the rotational degrees of freedom gain energy in the presence of the THz pulse, as illustrated in Fig. 1. The time structure of the pulse when it changes its polarization direction can still be seen in $\Delta\langle E_R\rangle$ in spite of the rotational averaging over initial conditions. As expected, no further change in total energy occurs after $t = 250$ fs, when the pulse is over.

In the dimer case, both $\Delta\langle E_R\rangle$ and $\Delta\langle E_T\rangle$ increase due to the THz pulse. However, the increase of translational energy of the monomers is, in this, case much smaller than that of rotational energy. On average, the dimer fragments in its two water molecule constituents very early during or shortly after the THz pulse, which closes the channel for energy transfer between rotational and translational motion by interactions between the monomers. Therefore, the relative translational mode between both centers of mass remains much colder than the individual rotational modes of both monomers, and equipartition cannot be reached. To understand the origin of the translational energy increase of the monomers we can first inspect the form of the interaction term between matter and radiation. In the non-polarizable water model considered here the interaction of the electric field with the system is simply the sum of the interactions with the individual dipole moments of the monomers

$$E^{w-EF} = -\sum_m \sum_{a_m} q_{a_m}(\mathbf{r}_{a_m} \cdot \mathbf{E}) = -\sum_m \boldsymbol{\mu}_m \cdot \mathbf{E}, \tag{4}$$

where $\mathbf{r}_{a_m}$ is the position of the a-th point charge of the m-th monomer, $\boldsymbol{\mu}_m$ is the permanent dipole moment of monomer m and $\mathbf{E}$ is the external electric field. This term has no *direct* effect on the translational motion of the centers of mass and only depends on the orientation of each individual dipole in the electric field. The total potential energy (E_P) of the system in the presence of the electric field consists of the sum of pair interactions between monomers and the interaction of each monomer with the field

$$E_P = E^{w-w}_{\text{pair}} + E^{w-EF}. \tag{5}$$

E^{w-w}_{pair} includes a Lennard-Jones term between each water molecule, which is spherically symmetric, and Coulombic interactions between each effective partial charge in each water molecule, which account for the effective charge distribution in the water model[39]. This last part of E^{w-w}_{pair} is strongly directional and is responsible for the adequate description of the coordination and H-bonding between water molecules. Hence, the rotation of the water monomers forced upon them by the electric field through E^{w-EF} results in unfavorable configurations due to the E^{w-w}_{pair} term, which leads to translational motion of the centers of mass of the monomers and to energy transfer between monomer rotations and translations. Higher order multipolar interaction terms than dipole-dipole are embedded in the E^{w-w}_{pair} term and are crucial to describe the properties of liquid water [44–47]. However, for the sake of argument let us consider for a moment a simplified model of permanent point dipoles. The

potential energy of a system of permanent point dipoles reads

$$E_{\text{pair}}^{d-d} = \sum_{i>j} -\frac{\mu_i \mu_j}{r_{ij}^3}(\cos\theta_{ij} - 3\cos\theta_i \cos\theta_j) \tag{6}$$

where r_{ij} is the distance between the centers of the two dipoles, θ_{ij} is the relative angle between the dipoles and θ_i and θ_j are the angles formed by the two dipoles with respect to the line connecting their centers. Since the dipole-dipole interaction term couples the relative orientation and relative distance of each pair of dipoles, an external electric field can transfer energy to the center of mass translational motion of the individual monomers via the indirect mechanism described above. In the case of aggregates of molecules with individual permanent dipoles, this constitutes the zeroth order mechanism for energy transfer from an external field to the relative translational motion of each constituent through their individual rotational degrees of freedom. Polarization effects are not considered at this level in such a mechanism. It should be emphasized that the pulse frequency of 3 THz is smaller by more than one order of magnitude than intramolecular vibrational modes of separate water monomers and about 5 times smaller than hindered librational modes of water monomers[48]. Hence, the interaction with the THz pulse occurs in a non-resonant fashion as a response to the instantaneous electric field amplitude.

The effect of an electric field on the preferred relative orientation between the two water monomers is clearly seen by inspecting the potential energy curve of the water dimer along the ∠HOO relative angle in Fig. 2. The potential energy curves correspond to the TIP4P/2005 water force-field used in the trajectory propagations. In the minimum energy configuration of the dimer, two water monomers orient themselves to form a H-bond. The applied static electric field is polarized along the x-axis, which is the direction of the H-bond in the minimum energy configuration of the dimer shown in Fig. 3(a). To construct the potential energy curves along the ∠HOO, the donor water molecule is rotated in the XZ plane around the y-axis. The potential energy curves were compared for static electric fields with amplitudes 0, 0.028, 0.087, 0.274 and 0.614 V/Å, which in the case of a pulse would correspond to intensities of 0, 10^{10}, 10^{11}, 10^{12} and 5×10^{12} W/cm^2. The change in the shape of the potential is the result of the relative magnitude of the terms E_{pair}^{w-w} and E^{w-EF} in Eq. 5. By changing the field amplitude from 0.274 V/Å to 0.614 V/Å, the shape of the potential energy curve changes significantly in comparison to lower amplitudes. Such high electric field is able to create a displaced and deep potential well along the relative orien-

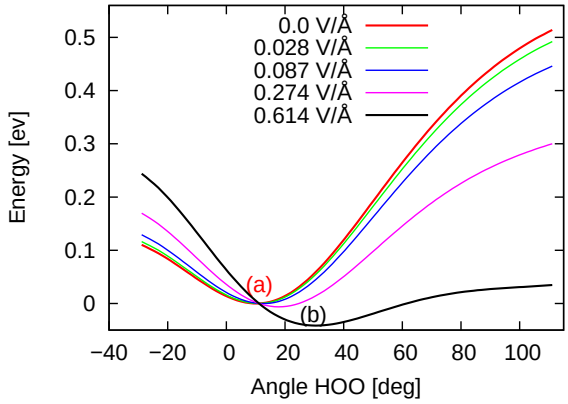

FIG. 2. Potential energy curve for HOO angle with different electric field amplitudes. The labels (a) and (b) correspond to the dimer configurations as shown in Fig. 3.

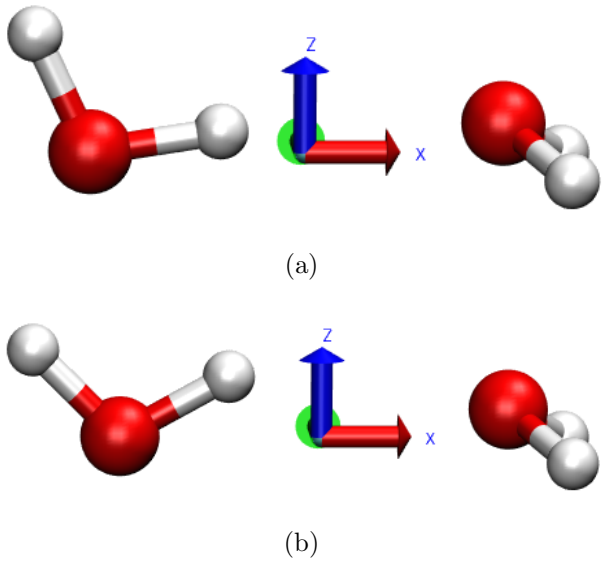

FIG. 3. Minimum energy configurations of the water dimer (a) without field and (b) with a field of 0.614 V/Å as presented in Fig. 2.

tation between the water molecules. At the high field amplitude, the electric field is strong enough to substantially alter the H-bond and bring the water molecules out of their preferred field free relative orientation. The time delay of about 100 fs in the rise of the translational component $\langle E_T \rangle$ compared to the start of the pulse and seen in Fig. 1 is related to the fact that the electric field has to reach a certain peak amplitude in order to disrupt the H-bond and push the water molecules into configurations for which their relative distance will start

to change.

The H-bond strength of the water dimer is 23.8 KJ/mol (≈ 0.25 eV)[49]. As a consequence, a certain threshold value ϵ_T for the external electric field amplitude is required in order to bring water molecules out of their preferred H-bond arrangements[15,17], as already seen in Fig. 2. The THz pulse can then be divided into different parts, depending on whether the electric field amplitude $\epsilon(t)$ is larger or smaller than the threshold value ϵ_T required to disrupt the H-bond structure. From Fig. 2 one can estimate ϵ_T to be of the order of 0.2 to 0.3 V/Å. Only when $\epsilon(t) > \epsilon_T$, which for the half cycle pulse of Eq. 1 is achieved only in the central oscillation, the electric field can effectively bring molecules out of their H-bond arrangements. This is the reason why, already for the dimer case, $\Delta\langle E_R\rangle$ increases mostly during the central pulse oscillation and hardly changes during the two side wings of smaller amplitude.

2. Water tetramer and larger clusters

For water clusters larger than the dimer the average number of H-bonds per water molecule increases from 1/2 to between 3 and 4. As may already be anticipated, this has profound consequences for the dynamics of energy increase and energy transfer in the clusters. Fig. 4 illustrates the total kinetic, rotational and translational energy increase for water clusters of sizes 4, 8, 32, 64 and finally bulk water at the same initial temperature of 200 K. This temperature was chosen to ensure equilibration of the clusters without evaporation (loss) of water molecules into their surroundings, which occurs at higher temperatures. There are various features of the energy intake dynamics that can now be understood on the basis of the observations made for the case of the water dimer. (i) Smaller clusters feature a larger energy increase immediately after the THz pulse because they have on average fewer H-bonds per monomer, as seen both in Figs. 4(a) and 4(c). (ii) $\Delta\langle E_R\rangle$ becomes increasingly delayed as the cluster size increases because the number of surface water molecules with fewer H-bonds decreases in relation to the cluster's volume. As a consequence, the time t_2, defined as the time of maximum energy gain becomes increasingly delayed for larger clusters. Exactly the same trend is observed for t_1, the time at which $\Delta\langle E_K\rangle$ starts increasing significantly. (iii) Equilibration between the $\Delta\langle E_R\rangle$ and $\Delta\langle E_T\rangle$ components (cf. Figs. 4(b) and 4(c)) is achieved for clusters with 32 and 64 water molecules, besides the bulk system.

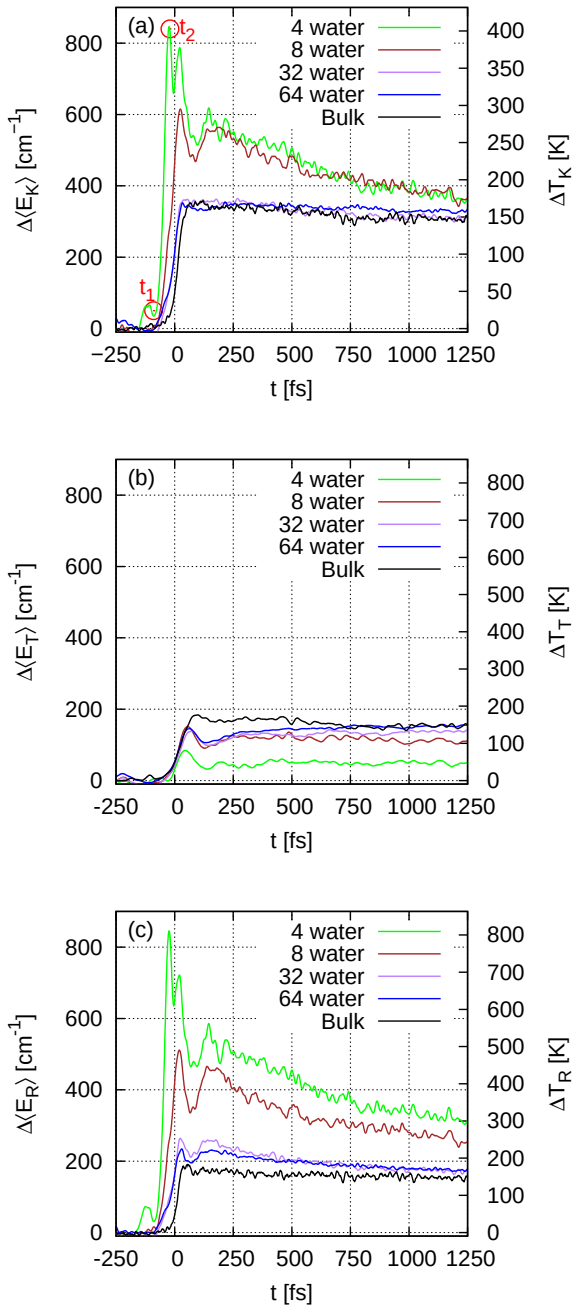

FIG. 4. (a) Ensemble averaged total kinetic energy increase ($\Delta\langle E_K\rangle$), (b) translational energy increase ($\Delta\langle E_T\rangle$) and (c) rotational energy increase ($\Delta\langle E_R\rangle$) for the water clusters of sizes 4, 8, 32 and 64 and for bulk water at 200 K. Red circles are showing the points t_1 and t_2 for 4 water cluster only. t_1 is the point when significant change happens in $\Delta\langle E_K\rangle$ and t_2 is the point when $\Delta\langle E_K\rangle$ is maximum.

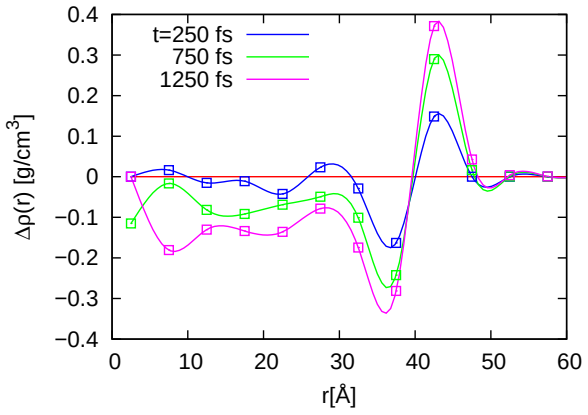

FIG. 5. Water density difference ($\Delta\rho$) with respect to the density at -250 fs (before the THz pulse) at times 250, 750 and 1250 fs in the presence of the THz pulse. r is the distance to the center of the spherical cluster.

For the smaller clusters with 4 and 8 water molecules, collisional energy transfer stops as the clusters start expanding, similarly as in the dimer case. (iv) The total kinetic energy $\Delta\langle E_K\rangle$ decreases after the pulse for the smaller clusters. Since the total energy of each cluster is conserved after the pulse, the total kinetic energy decrease corresponds to an increase in the relative potential energy between monomers as the small clusters expand. This can be thought of as a sort of evaporative cooling taking place at the surface of the clusters as outer water molecules leave the cluster after interaction with the THz pulse.

3. Inertial confinement in ultrafast heated clusters

In earlier investigations on liquid water interacting with the THz pulse at a density of 1 g/cm^3, constant volume had been assumed[36,37]. This rests on the assumption that the number of water molecules in the region interacting with the THz pulse remains constant, or in other words, there is no substantial expansion of the system during and after the interaction with the THz pulse in the time scales of interest. As an indication that this may be the case, we already saw in the previous section that at least the total energy gain converges to the bulk value for clusters with a few tens of water molecules. Here we investigate this assumption in more detail on the basis of force-field treatment of water, such that several thousand water molecules can be taken into account. The dynamics of an isolated spherical cluster of radius 40 Å and 8843 water molecules, which was extracted from

a thermally equilibrated periodic box of liquid water at 300 K, were simulated in the presence of the THz pulse. The initial density in the interior of the cluster was set to 1 g/cm^3.

The density as a function of the distance to the center of the cluster was calculated by binning the radial coordinate in spherical shells of width 5 Å at times −250 (before the pulse), 250, 750 and 1250 fs relative to the center of the THz pulse. As seen in Fig. 5, the density varies the most in the outer 5 to 10 Å shell, which diffuses out by also 5 to 10 Å. The density in the inner regions of the cluster remains quite stable, decreasing by about 0.15 g/cm^3 during the first picosecond after the pulse. Larger clusters may still lead to a more effective inertial confinements, and it appears justified to assume a constant density in simulations of heated bulk water at the time scales of interest.

B. THz pulse interaction with bulk water

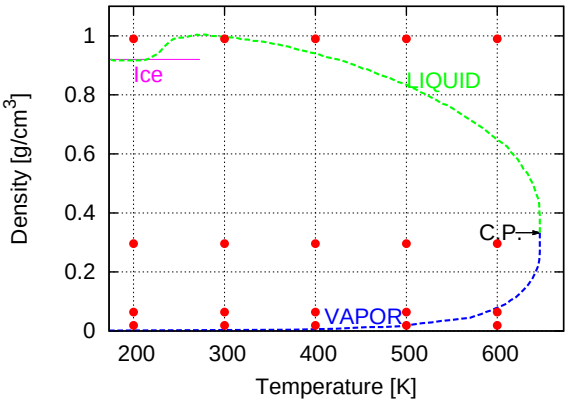

FIG. 6. Temperature (T)-density (ρ) phase diagram of water. C.P. is the critical point. Red dots are the states of water in the phase diagram that have been used to explore the effect of THz pulse.

We have discussed above how an intense, sub-cycle THz pulse interacts with an isolated water molecule and with water clusters of various sizes. Summarizing, an isolated water molecule interacts with the pulse through its permanent dipole moment thus gaining a large amount of rotational energy. Only when several water molecules are in close proximity can part of the rotational energy be transformed into relative translational energy owing to the coupling between rotational and relative translational motion of the water monomers in the cluster.

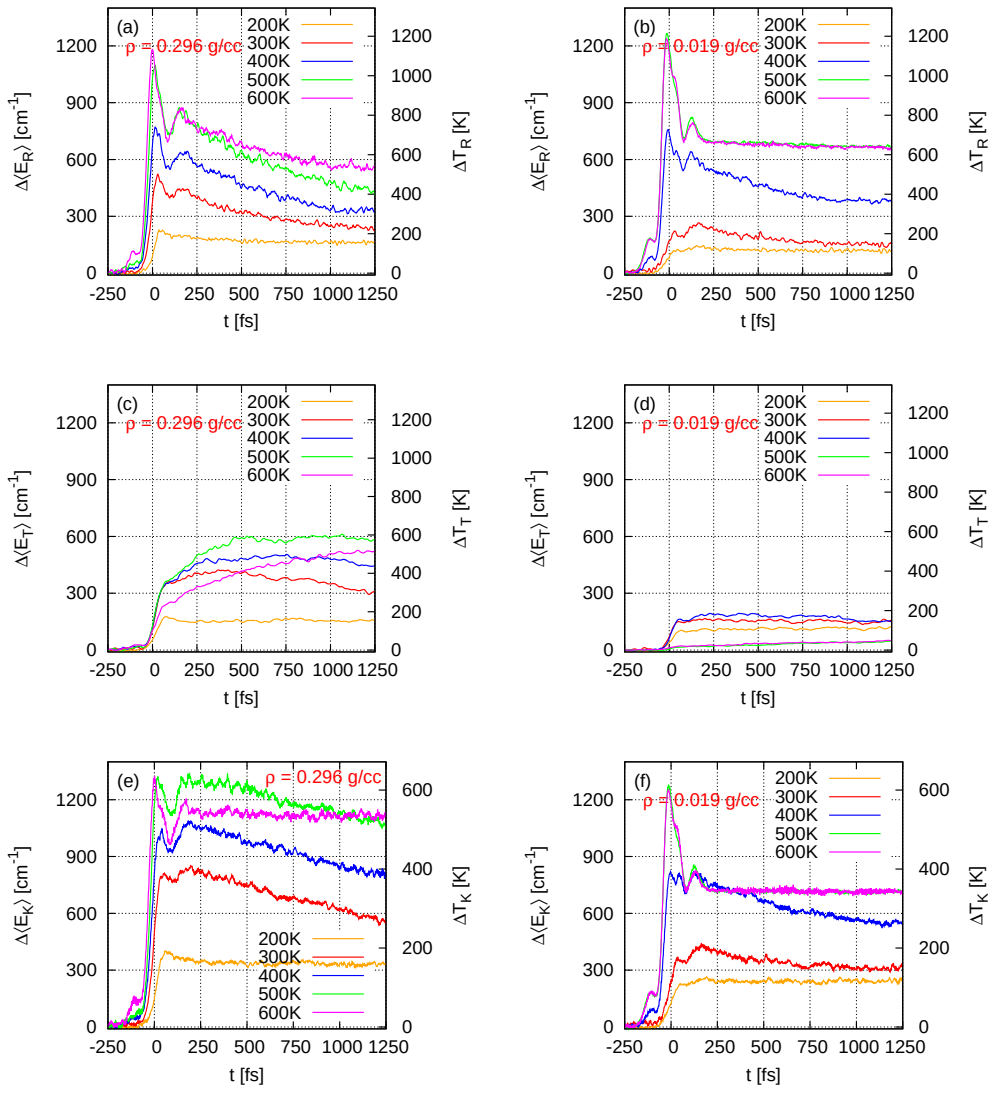

FIG. 7. Total kinetic energy ($\Delta\langle E_K\rangle$), translational energy ($\Delta\langle E_T\rangle$) and rotational energy ($\Delta\langle E_R\rangle$) per water molecule at different temperatures for densities 0.296 g/cm^3 (a,c,e) and 0.019 g/cm^3 (b,d,f).

In the following, we explore the interaction of the THz pulse and the subsequent energy transfer dynamics in bulk water at different constant densities and equilibrated at different initial temperatures. Regarding initial temperature, this parameter is easily controllable in experimental realizations. As for density, we have already shown that, on the time scales of interest, the inner part of the cluster remains at its initial density during the interaction with the pulse and is inertially confined by the outer shell. Therefore, simulations at the constant

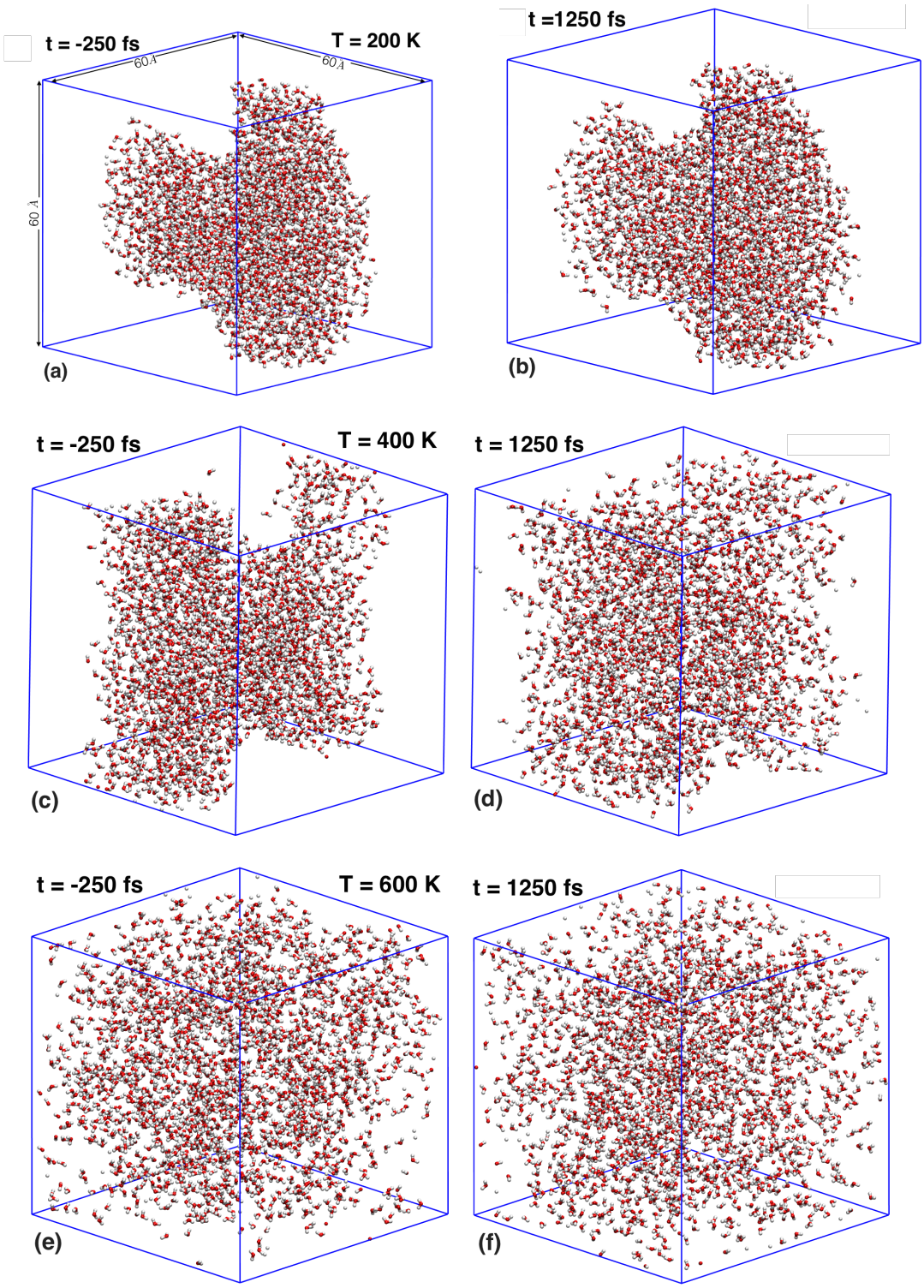

FIG. 8. Snapshots of simulation boxes with density 0.3 g/cm^3 and different temperatures (T= 200 K, 400 K and 600 K) before the pulse, $t = -250$ fs (a,c,e) and after the pulse, $t = 1250$ fs (b,d,f).

density (i.e. constant volume) of the liquid phase, 1 g/cm^3, are justified. Moreover, the macroscopic density under real physical confinement of the interaction volume by e.g. hard walls can be maintained during and after the heating-up process. Therefore, we consider various densities ranging from very low up to normal liquid density. Depending on the density and initial temperature of the confined system in equilibrium, the aggregation state of water may vary from gas phase to liquid or amorphous solid phases and the coexistence of the two. This is illustrated in the saturation diagram of pure water shown in Fig. (6)[50]. In the regions inside the curve vapor and liquid water coexist. Outside the curve only one phase is present, either water vapor or condensed water. The dynamics of energy transfer from the THz pulse and the subsequent energy redistribution among rotational and translational degrees of freedom are strongly dependent on the possible aggregation states found in the diagram. Those initial conditions at which simulations have been performed in this work are marked with a red dot in Fig. (6).

There are three distinctive features of the heating-up dynamics of water clusters that vary strongly as a function of the size of the cluster. *First*, for isolated water molecules and for clusters up to 8 monomers the amplitude profile of the THz pulse is imprinted in the rotational energy of the water molecules. This is indicative of none or few hydrogen bonds per monomer as compared to the bulk or to larger clusters. As a consequence, water molecules are rotationally accelerated and shortly thereafter slowed down in the presence of the THz field before they can have significant collisions with neighboring monomers. This can be observed in Figs. 1 and 4c. *Second*, an equilibriation between the rotational and translational components of the kinetic energy is only achieved for clusters after a certain minimum size. In our simulations we find equilibriation between rotational and translational energy components for clusters of 32 or more water molecules. Smaller clusters fragment before equilibriation through collisions can complete. An extreme example of this corresponds to the water dimer and tetramer. *Third*, the total kinetic energy of the clusters with four and eight monomers decreases during the first picosecond as the clusters expand, which is mirrored by the corresponding increase of potential energy as the monomers separate from each other against attractive electrostatic interactions. This effect is not observed for larger aggregates, which mostly maintain their structure.

These basic features can be recognized when letting bulk water interact with the THz pulse at different densities and initial temperatures. Snapshots of 2048 water molecules

at a density of 0.296 g/cm^3 for different initial temperatures of 200, 400 and 600 K are shown in Fig. 8. The system at 200 K corresponds essentially to a piece of amorphous ice with small internal energy. The system at 400 K is made of a large droplet of hot liquid water with smaller clusters and monomers surrounding it in the vapor state, whereas the system at 600 K is made of almost homogeneously distributed water molecules with a large mobility and collisional rate. This leads immediately to very different heating-up dynamics. The colder system gains in total less energy due to the more hindered water monomers. The equilibration between rotational and translational energy is however almost instantaneous due to the tight interactions between the monomers. As the temperature increases the amplitude profile of the THz pulse manifests more strongly in the rotational energy component because the interactions between neighboring water molecules become progressively weaker, as seen in Fig. 7a. Another consequence of larger temperatures is that the energy transfer between the rotational and translational components of the kinetic energy is not instantaneous anymore as compared to colder temperatures (cf. Figs. 7c and 7d). The slowest energy transfer to translational motion occurs at 600 K as a consequence of the larger separation and weaker interactions between water molecules. A decrease of the total kinetic energy shortly after the pump pulse occurs for systems initially between 300 and 500 K due to substantial evaporation of monomers from the outer shells of the liquid portion. This can be seen by comparing the snapshots in Figs. 10a, 10c and 10e with those in Figs. 10b, 10d and 10f, respectively.

As compared to the previous examples, a reduced density of 0.019 g/cm^3 leads to differences mostly for the high temperature cases. At T= 500 K and T=600 K the water molecules are homogeneously distributed across the available volume and at a large average distance from one another. This results in dynamics of the rotational degrees of freedom similar to those of isolated monomers and characterized by a slow rate of energy transfer to translational degrees of freedom due to infrequent collisions. This can be seen by comparing the increase of translational energy shown in Figs. 7c and 7d. At this density, only the colder systems at T= 200 K and T= 300 K achieve energy equipartition between rotational and translational degrees of freedom because most of the water molecules are condensed forming ice and liquid droplets, as seen in Figs. 10c and 10e. This leads to coupled hindered rotational and translational motion in the condensed phase and the corresponding fast energy transfer.

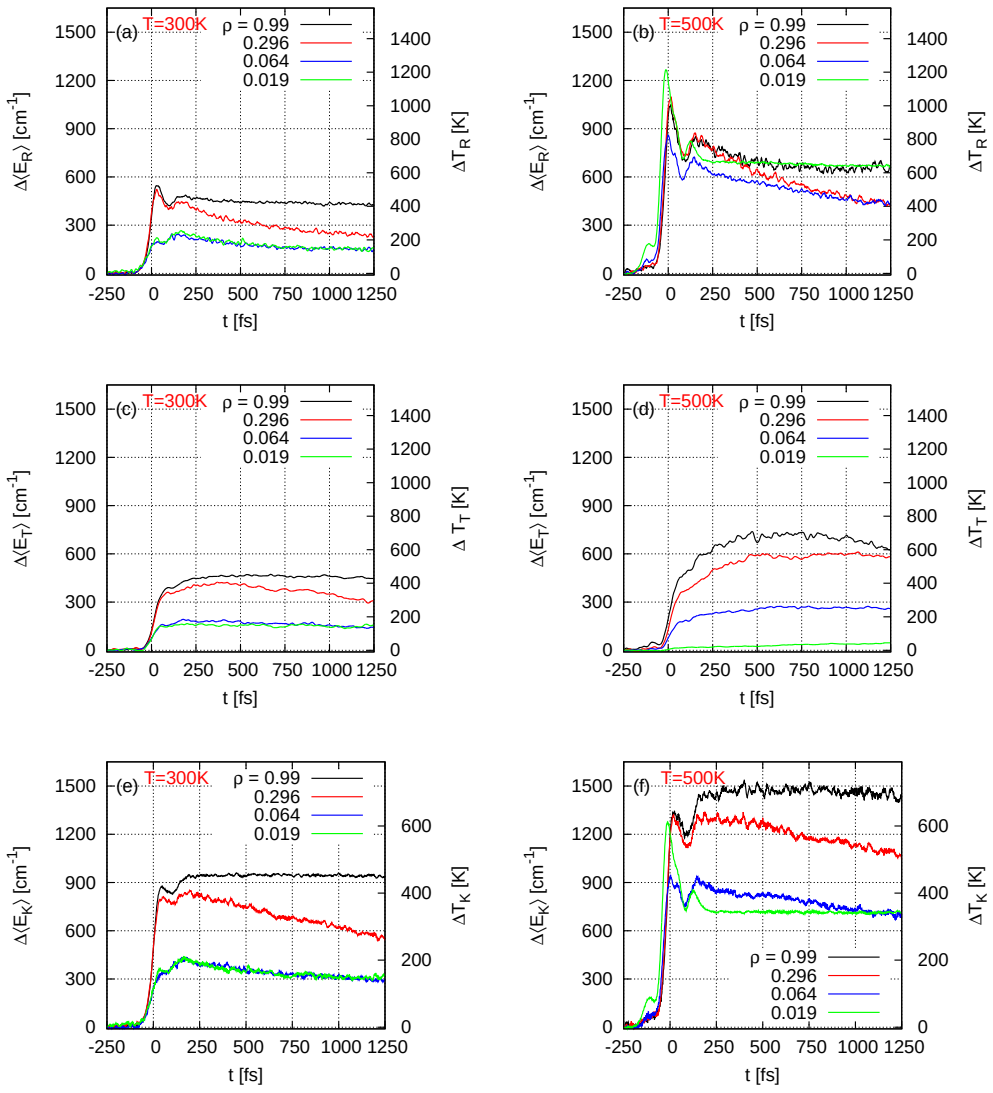

FIG. 9. Total kinetic energy ($\Delta\langle E_K\rangle$), translational energy ($\Delta\langle E_T\rangle$) and rotational energy ($\Delta\langle E_R\rangle$) per water molecule at different densities (in g/cm^3) for initial temperatures 300 K (a,c,e) and 500 K (b,d,f) of the system.

At temperatures T=500 K and T=600 K the amount and rate of energy transfer from the THz pulse to rotational motion is relatively independent of the density of the system, as can be seen in Fig. 9b. Independently of the density, the high temperatures result in weak hydrogen bonding and the rotational degrees of readily respond to the THz pulse. However, the collisional energy transfer from the rotational to the translational degrees of freedom at these high temperatures is strongly dependent on the density of the system, as illustrated in

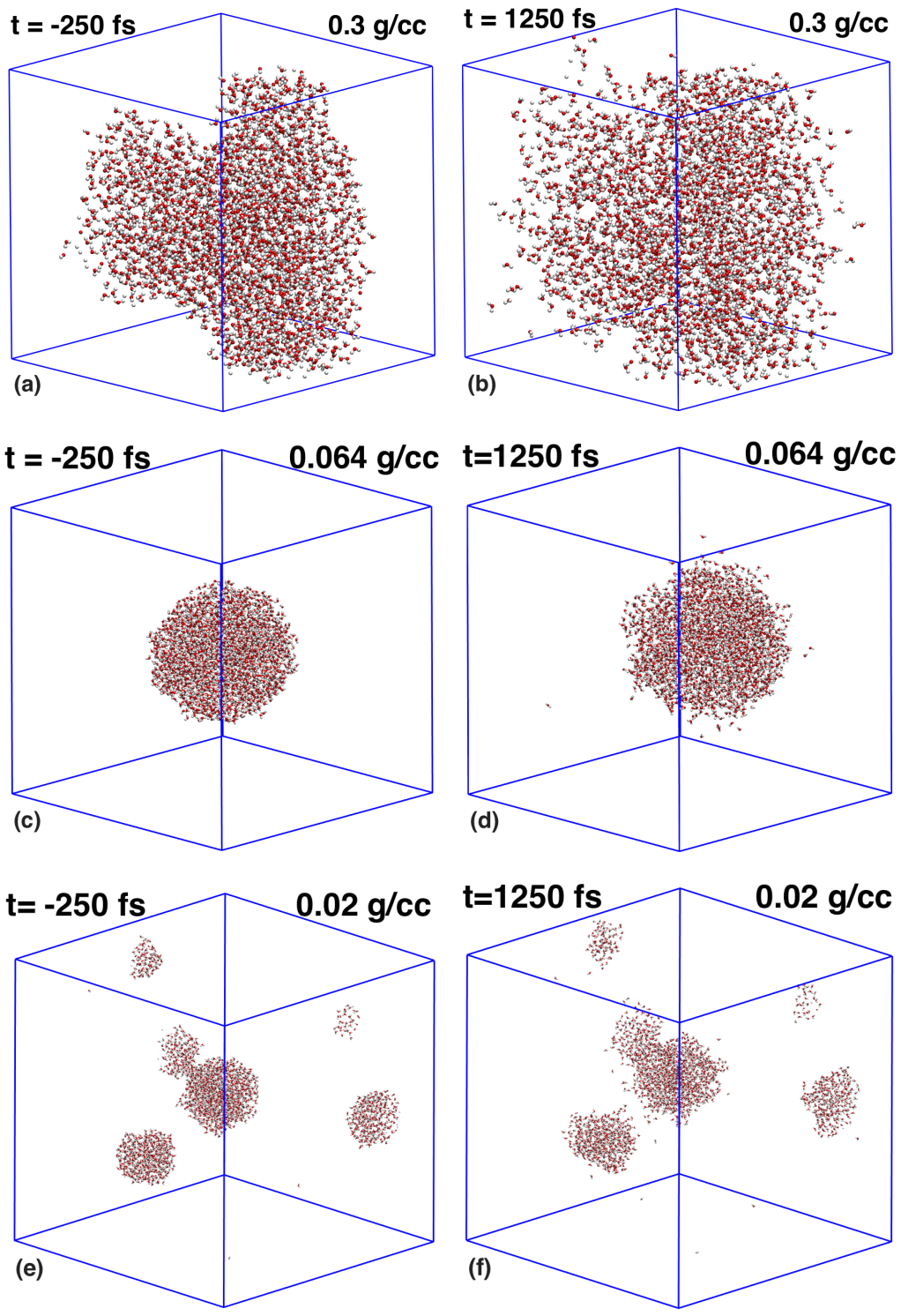

FIG. 10. Snapshots of water systems at T=300 K and different densities (0.3 g/cm^3, 0.064 and 0.02 g/cm^3) before the pulse, $t = -250$ fs (a,c,e) and after the pulse, $t = 1250$ fs (b,d,f).

Fig. 9d. At low densities almost no collisions occur whereas at 1 g/cm^3 the rotational and

translational temperatures are equilibriated within 1 ps.

As a final remark, the simulations of the interaction of the THz pulse with liquid water at an initial temperature of 300 K and density of 1 g/cm^3 can be compared with our previous *ab initio* molecular dynamics results[36,37]. The total kinetic energy increase $\Delta\langle E_K\rangle$ per water monomer is found to be about a factor 2 larger in the *ab initio* case than with the present rigid force-field approach. The main difference is related to the direct energy intake of the internal vibrational degrees of freedom of the water monomers during the THz pulse and which is related to polarization effects not captured by rigid force-fields. The mechanism of energy transfer to rotational and translational degrees of freedom remains however the same and the amount of energy transferred to these modes is in both types of simulations qualitatively agrees to within 20%.

IV. CONCLUSION

We have discussed in detail the mechanisms by which a highly intense (5×10^{12} W/cm^2) and ultrashort (fwhm 141 fs) THz pulse couples to clusters of water molecules and to bulk water and transfers a large amount of energy to the system. The fundamental coupling mechanism between the THz pulse and the water molecules is through the permanent dipole moment of those with the electric field component of the pulse. Therefore, the THz pulse transfers energy only to rotational motion of isolated water molecules and translational motion of the center of mass remains unaffected due to electrical neutrality of the molecules. For clusters with two or more molecules, coupling between hindered rotations and translations exists and the translational motions also gain energy during and after interaction with the THz pulse. Inspection of the potential energy curve of the $\angle$OOH angle of the water dimer in the presence of a static electric field shows small changes for a electric field amplitude up to 0.087 V/Å. Beyond this field strength, a small variation in the electric field will induce a significantly large change in the potential energy curve. At a electric field amplitude of 0.614 V/Å, the potential energy curve shows that the electric field can break the hydrogen bond in the water dimer and bring the permanent dipole moments of the two monomers to orient with the polarization axis of the electric field.

We studied the interaction of confined water at well defined initial temperature and different densities. Even relatively small clusters lead to inertial confinement of the water

molecules below the most external shells, which justifies investigations of bulk water at constant density of 1 g/cm^3. We also investigated lower densities, which can result from physical confinement either by macroscopic physical walls or even in nanostructures. High temperatures of 500 and 600 K lead to rotational dynamics similar to isolated water molecules. Lower temperatures, in which the interactions between water monomers are stronger, lead to a smaller energy transfer from the THz pulse. The density of the system plays a key role in the collisional energy transfer between rotational and translational motion. For large temperatures, a large density leads to a high collision rate and quick equilibriation whereas a small density prevents collisions and no equilibriation can occur. For small temperatures, a large fraction of the system is in a condensed state and equilibriation between rotational and translational motion occurs almost instantaneously.

These results constitute a relevant step towards studies of thermally activated chemical and biological processes, in which the water medium can be used as a channel to deliver the energy of a THz pump pulse to the molecules of interest. The trends identified in terms of temperature and density of the system open the door to the design of strategies in which the heating-up rate of substances dissolved in water can be controlled by such thermodynamic parameters.

ACKNOWLEDGMENTS

We are grateful to the Virtual Institute of the Helmholtz Association "Dynamic Pathways in Multidimensional Landscapes" for financial support.

REFERENCES

[1]J. D. Smith, C. D. Cappa, K. R. Wilson, R. C. Cohen, P. L. Geissler, and R. J. Saykally, Proc. Natl. Acad. Sci. **102**, 14171 (2005).

[2]E. Schwegler, G. Galli, and F. m. c. Gygi, Phys. Rev. Lett. **84**, 2429 (2000).

[3]D. H. Jung, J. H. Yang, and M. S. Jhon, Chem. Phys. **244**, 331 (1999).

[4]A. M. Saitta, F. Saija, and P. V. Giaquinta, Phys. Rev. Lett. **108**, 207801 (2012).

[5]E. Dahl, Water Res. **10**, 677 (1976).

[6]R. Zangi and A. E. Mark, J. Chem. Phys. **119**, 1694 (2003).

[7]R. Evans and U. Marini Bettolo Marconi, J. Chem. Phys. **86**, 7138 (1987).

[8]P. Hirunsit and P. B. Balbuena, J. Phys. Chem. C **111**, 1709 (2007).

[9]J. Martí and M. C. Gordillo, Phys. Rev. E **64**, 021504 (2001).

[10]M. Gordillo and J. Mart, Chem. Phys. Letters **329**, 341 (2000).

[11]J. C. Rasaiah, S. Garde, and G. Hummer, Annu. Rev. Phys. Chem. **59**, 713 (2008).

[12]S. A. Clough, Y. Beers, G. P. Klein, and L. S. Rothman, J. Chem. Phys. **59**, 2254 (1973).

[13]P. L. Silvestrelli and M. Parrinello, Phys. Rev. Lett. **82**, 3308 (1999).

[14]A. Vegiri, J. Chem. Phys. **116**, 8786 (2002).

[15]Y. C. Choi, C. Pak, and K. S. Kim, J. Chem. Phys. **124**, 094308 (2006).

[16]A. Vegiri and S. V. Schevkunov, J. Chem. Phys. **115**, 4175 (2001).

[17]D. Rai, A. D. Kulkarni, S. P. Gejji, and R. K. Pathak, J. Chem. Phys. **128**, 034310 (2008).

[18]U. Buck, I. Ettischer, M. Melzer, V. Buch, and J. Sadlej, Phys. Rev. Lett. **80**, 2578 (1998).

[19]S. V. Shevkunov and A. Vegiri, J. Mol. Struct.: THEOCHEM **574**, 27 (2001).

[20]J. K. Gregory, D. C. Clary, K. Liu, M. G. Brown, and R. J. Saykally, Science **275**, 814 (1997).

[21]D. Lockhart and P. Kim, Science **257**, 947 (1992).

[22]K. J. Freedman, M. Jürgens, A. Prabhu, C. W. Ahn, P. Jemth, J. B. Edel, and M. J. Kim, Anal. Chem. **83**, 5137 (2011).

[23]M. A. Fox and E. Galoppini, J. Am. Chem. Soc. **119**, 5277 (1997).

[24]S. Franzen, R. F. Goldstein, and S. G. Boxer, J. Phys. Chem. **94**, 5135 (1990).

[25]A. Gopher, Y. Blatt, M. Schönfeld, M. Okamura, G. Feher, and M. Montal, Biophys. J . **48**, 311 (2015).

[26]H. J. Bakker, S. Woutersen, and H. K. Nienhuys, Chem. Phys. **258**, 233 (2000).

[27]O. Link, E. Vöhringer-Martinez, E. Lugovoj, Y. Liu, K. Siefermann, M. Faubel, H. Grubmller, R. B. Gerber, Y. Miller, and B. Abel, Faraday Discuss. **141**, 67 (2009).

[28]R. Shimano, S. Watanabe, and R. Matsunaga, J Infrared Milli Terahz Waves **33**, 861 (2012).

[29]K. F. Rinne, S. Gekle, D. J. Bonthuis, and R. R. Netz, Nano Lett. **12**, 1780 (2012).

[30]S. Imoto, S. S. Xantheas, and S. Saito, J. Phys. Chem. B (2015).

[31]S. Woutersen and H. J. Bakker, Nature **402**, 507 (1999).

[32]S. Woutersen, U. Emmerichs, and H. J. Bakker, Science **278**, 658 (1997).

[33]S. Woutersen, U. Emmerichs, and H. J. Bakker, Science **278**, 658 (1997).

[34]J. Hasted, S. Husain, F. Frescura, and J. Birch, Chem. Phys. Lett. **118**, 622 (1985).

[35]N. Huse, S. Ashihara, E. T. Nibbering, and T. Elsaesser, Chem. Phys. Lett. **404**, 389 (2005).

[36]P. K. Mishra, O. Vendrell, and R. Santra, Angew. Chem. Int. Ed. **52**, 13685 (2013).

[37]P. K. Mishra, O. Vendrell, and R. Santra, J. Phys. Chem. B **119**, 8080 (2015).

[38]C. Vicario, B. Monoszlai, and C. P. Hauri, Phys. Rev. Lett. **112**, 213901 (2014).

[39]J. L. F. Abascal and C. Vega, J. Chem. Phys. **123**, 234505 (2005).

[40]S. Plimpton, J. Comput. Phys. **117**, 1 (1995).

[41]D. J. Evans and B. L. Holian, J. Chem. Phys. **83**, 4069 (1985).

[42]S. Nosé, Mol. Phys. **57**, 187 (1986).

[43]J.-P. Ryckaert, G. Ciccotti, and H. J. Berendsen, Journal of Computational Physics **23**, 327 (1977).

[44]J. L. F. Abascal and C. Vega, J. Phys. Chem. C **111**, 15811 (2007).

[45]S. Niu, M.-L. Tan, and T. Ichiye, J. Chem. Phys. **134**, 134501 (2011).

[46]G. N. Patey and J. P. Valleau, J. Chem. Phys. **64**, 170 (1976).

[47]C. Vega and P. A. Monson, J. Chem. Phys. **102**, 1361 (1995).

[48]M. Heyden, J. Sun, S. Funkner, G. Mathias, H. Forbert, M. Havenith, and D. Marx, Proc. Natl. Acad. Sci. **107**, 12068 (2010).

[49]T. Urbic, Chem. Phys. Lett. **610611**, 159 (2014).

[50]W. Wagner and A. Pruß, J. Phys. Chem. Ref. Data **31**, 387 (2002).